3D integral microscopy based in far-field detection

G. Scrofani, J. Sola-Pikabea, A. LLavador, E. Sánchez-Ortiga, J. C. Barreiro, et al.

G. Scrofani, J. Sola-Pikabea, A. LLavador, E. Sánchez-Ortiga, J. C. Barreiro, J. Garcia-Sucerquia, N. Incardona, M. Martinez-Corral, "3D integral microscopy based in far-field detection ," Proc. SPIE 10666, Three-Dimensional Imaging, Visualization, and Display 2018, 106660Z (19 June 2018); doi: 10.1117/12.2304330

SPIE.

Event: SPIE Commercial + Scientific Sensing and Imaging, 2018, Orlando, Florida, United States

3D INTEGRAL MICROSCOPY BASED IN FAR-FIELD DETECTION

G. Scrofani[a], J. Sola-Pikabea[a], A. Llavador[a], E. Sanchez-Ortiga[a], J.C. Barreiro[a], J. Garcia-Sucerquia[b], N. Incardona[a], and M. Martnez-Corral[a]

[a]Department of Optics, University of Valencia, E-46100 Burjassot, Spain
[b]Universidad Nacional de Colombia, Sede Medellin, School of Physics, A.A. 3840 Medelln 050034, Colombia

ABSTRACT

Lately, Integral-Imaging systems have shown very promising capabilities of capturing the 3D structure of microscopic and macroscopic scenes. The aim of this work is to provide an optimal design for 3D-integral microscopy with extended depth of field and enhanced lateral resolution. By placing an array of microlenses at the aperture stop of the objective, this setup provides a set of orthographic views of the 3D sample. Adopting well known integral imaging reconstruction algorithms it can be shown that the depth of field as well as spatial resolution are improved with respect to conventional integral microscopy imaging. Our claims are supported on theoretical basis and experimental images of a resolution test target, and biological samples.

Keywords: Fourier Plane Integral Microscopy, FiMic, Light Field

1. INTRODUCTION

In 1908 Gabriel Lippmann[1] reported a new technique, named as Integral Photography (IP), to capture perspective information of 3D scenes. The concept of plenoptic function, related to IP, was introduced in 1992 by Adelson and Wang.[2] It is a representation of the radiance of a given point as a function of its angle and position in the space. The IP concept was applied to microscopy first by Jang and Javidi,[3] aiming to display the microscopic images. Later, Levoy et al.[4] made an important contribution adapting to microscopy the concept of plenoptic function. In the case of microscopy, the most important issue is to preserve the resolution of the conventional microscope. Therefore, researchers are focusing their efforts in exploring new deconvolution tools, the use of 4D interpolation, and ultimately interpolation by time multiplexing.[5] In contrast, here we are reporting a fully-optical solution that solves problems of vignetting, resolution and low amount of pixels dedicated to each of the perspective. The key point is to place the microlens array (MLA) at the Fourier plane, in other words the aperture stop of a microscope objective. For this reason we adapted the previous name Integral Microscopy (iMic) to the new feature of our design, Far-field Integral Microscopy (FiMic). A proof of concept of FiMic was firstly published in.[6] Here we present a step forward in the design in terms of assembly of the microscope itself, and in terms of the formalism that describe its behavior with different parameter setups.

2. SYSTEM DESIGN

In FiMic the MLA is placed at the aperture stop (AS) of the microscopic objective (MO), this leads to directly capture a different elemental image (EI) at the sensor plane, behind each microlens of the array. The angular sampling that let us capture the plenoptic field is done at the AS by the multiplexing MLA. This set-up is shown in Fig.1. It is composed of five optical elements: one MO, two lenses RL1 and RL2, a MLA and a field-stop (FS). Ideally, in a fully custom design, the number of elements are reduced to two. Only MO and the MLA would be necessary. Since the AS is not accessible and the MLAs available in the market are limited, we: 1) conjugated the AS and the MLA thanks to a afocal relay system (RL1 and RL2); 2) limited the field of view with a field stop (FS), to obtain tangent EIs on the sensor. Being the FS placed at the focal distance from both RL1 and

Further author information: (Send correspondence to G. Scrofani)
E-mail: scrofani@uv.es

Three-Dimensional Imaging, Visualization, and Display 2018, edited by Bahram Javidi, Jung-Young Son, Osamu Matoba, Manuel Martinez-Corral, Adrian Stern, Proc. of SPIE Vol. 10666, 106660Z
 · doi: 10.1117/12.2304330

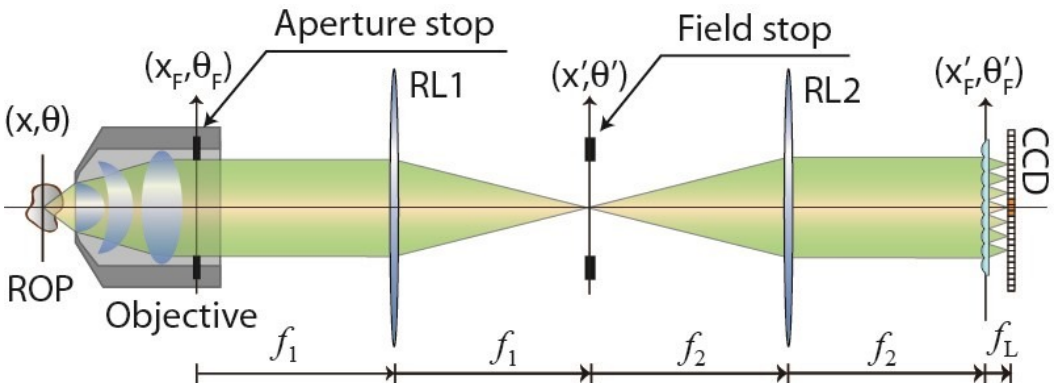

Figure 1. Schematic of Far-field integral microscope (FiMic). The reference object plane (ROP) is directly focusing on each of the orthographic views or EIs.

RL2 distances, the optimum is obtained when the size of the FS is chosen so that the field of view in the sensor matches the MALs pitch (p). The MLA conjugated at the AS let the FiMic design to sample angularly the specimen. Each different angular sample provides with one EI. This sampling is done at the AS by the MLA that divides de diameter of the AS ϕ_{AS} in N subapertures on both the orthogonal directions, with N being the number of microlenses that fit in the ϕ_{AS}. It can be calculated as $N = \phi_{AS}/p'$ with $p' = pf_1/f_2$. Consider that placning a number N of microlenses along de diameter of the AS correspond to an actual reduction of the host microscope effective NA (NA_H host microscope) of the same amount N. This implies that the performances of the microscope will be affected in therms of resolution and depth of field (DOF). So, let us look into detail on how resolution and DOF are affected. The resolution of each EI is determined by the wave-optics theory and the Nyquist sampling theorem. Considering wave-optics, one would say that two points must be separated of $\rho \geqslant N\lambda/2(NA_H)$, where $NA_H = \phi_{AS}/2f_{MO}$ is the numerical aperture of the microscope objective. Furthermore, the Nyquist sampling theory tells us that to distinguish two points, their distance must be at least the size (δ) of one pixel of the sensor $\rho \geqslant \delta f_2 f_{MO}/f_1 f_L$. The final resolution will be the maximum value between wave-optics and Nyquist resolution limit

$$\rho_{FiMic} \geqslant max\left\{N\frac{\lambda}{2NA_H}, 2\delta\frac{f_2 f_{MO}}{f_1 f_L}\right\} \tag{1}$$

The pixel size δ, must be chosen so that these two elements are equal. To calculate the depth of field the formulae of the DOF[7] must be rearranged to our sampled numerical aperture NA_H/N

$$DOF_{FiMic} = \lambda\frac{N^2}{NA_H^2} + \delta\frac{N}{NA_H^2}\frac{f_2 f_{MO}}{f_1 f_L} \tag{2}$$

If now we substitute the value of ρ in Eq. (2) the DOF obtained is

$$DOF_{FiMic} = \frac{5}{4}\frac{\lambda}{NA_H^2}N^2 \tag{3}$$

To understand the impact of the improvement we must compare performances in terms of resolution and DOF with the previous design, the iMic. In iMic, the MLA pitch determines those features, as the microlenses are the corresponding elements for the pixels in FiMic configuration. Differently than FiMic, with iMic it is necessary to compute the EIs, and referring to those, we will now show the lateral resolution and the DOF. Lateral resolution as calculated in[4] will be:

$$\rho_{iMic} \geqslant max\left\{\frac{\lambda}{2NA_H}, 2\frac{p}{M_H}\right\} = \mu\frac{\lambda}{NA_H} \tag{4}$$

Here M_H is the magnification of the MO coupled with the tube lens and $\mu = p/(\lambda/2NA_H)$ is the ratio of the MLA pitch and wave optic resolution limit. The DOF is

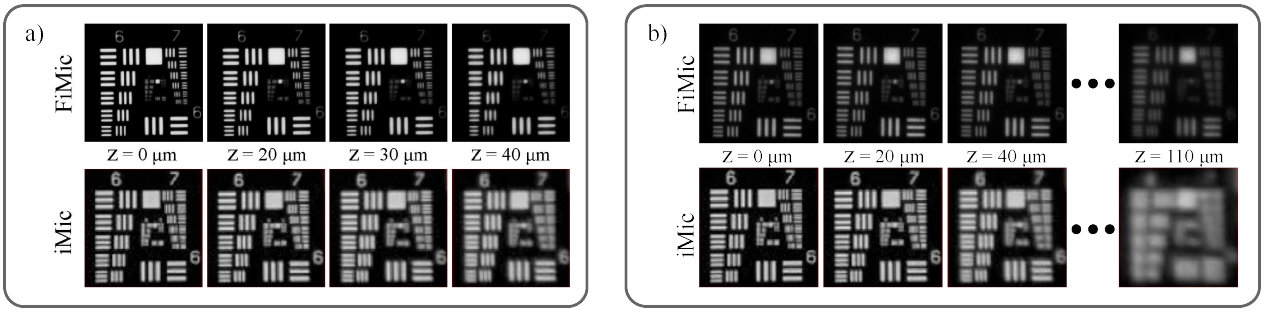

Figure 2. a) Central view shown of FiMic and iMic working with the same DOF. b) Central EIs of both microscopes working with the same resolution.

$$DOF_{iMic} = \frac{\lambda}{NA_H^2} + \frac{\mu p}{M_H NA_H} = \left(1 + \frac{\mu^2}{2}\right) \frac{\lambda}{NA_H^2} \tag{5}$$

Combining both resolution and DOF formulas for FiMic Eqs.(1),(3) and iMic Eqs.(4),(5) we get

$$\rho_{FiMic} = \frac{N}{1\mu} \rho_{iMic} \tag{6}$$

and

$$DOF_{FiMic} = \frac{5N^2}{4 + 2\mu^2} DOF_{iMic} \tag{7}$$

What these equations tell us is that for any configuration of iMic there will always be a FiMic that can: 1) have same resolution but higher DOF; 2) have same DOF but with better resolution; 3) bring to a trade-off with both improved resolution and DOF. These better performances are obtained at the price of lower angular sampling, that is to say, that the number of orthographic views is lower, but still sufficient for application of standard light-field algorithms such as refocusing and depth-map estimation.

3. SYSTEM BEHAVIOUR

To prove the previous statements regarding superior performances of FiMic over iMic we have built an iMic with $6.2\mu m$ of lateral resolution and $80\mu m$ DOF. Then two experiments where developed: in the first one FiMic was set to have 80m DOF and better resolution is shown; in the second FiMic was designed with the same resolution of $6.2\mu m$ in this way it can be proven that DOF is greater.

3.1 Same DOF experiment

In this experiment, we chose the elements of FiMic in order to obtain the same DOF of iMic, and see how lateral resolution is improved. The elements are: a microscope objective corrected to infinity with $f_{MO} = 10mm$ and $NA_{MO} = 0.5$ and $\phi_{AS} = 10mm$; the relay system composed of RL1 with $f_1 = 200mm$ and RL2 with $f_2 = 100mm$; a MLA with $f_L = 6.5mm$, $p = 1.0mm$, and $NA_{MLA} = 0.77$ (APH-Q-P1000-R2.95 manufactured by AMUS); the sensor is a 5-MegaPixel CMOS camera with pixel size $\delta = 2.2\mu m$. Considering the magnification power of the relay system, we can calculate N=5 as the number of microlenses that fit in the diameter of the aperture stop of the MO. Following the Eqs. (1) and (3) the system should provide with $\rho_{FiMic} = 3.4\mu m$ and $DOF_{FiMic} = 77\mu m$. Fig.2 shows the central view of both microscopes. To confirm the lateral resolution, as well as to show the DOF, an USAF resolution test chart was used. We axially displaced the test from the reference object plane (ROP) of steps of 10 μm up to $Z = \pm 40\mu m$. For each step an image was captured with both iMic and FiMic systems and the resulting central views for both can be seen in Fig. 2-(a). Only positive values of Z are shown because negative values behave equally. In Fig. 2-(a) it is possible to see the superior spatial resolution of FiMic that reaches $\rho_{FiMic} = 3.9\mu m$, performing better than the $6.2\mu m$ reached by iMic. This improvement in resolution can be explained by the low number N in this setup, witch reduces by the same factor the resolution of the MO.

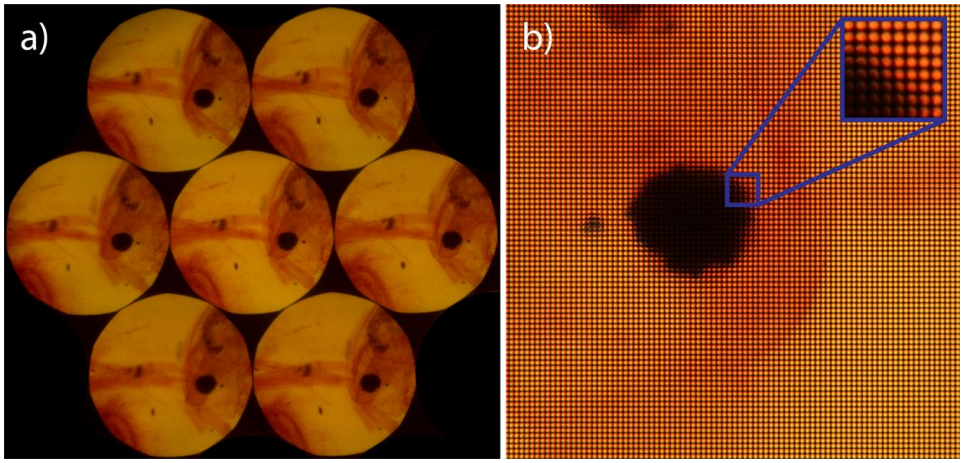

Figure 3. a) Elemental images directly recorded in FIMic. b) Microimages captured with iMic, from those it is possible compute the EIs.

3.2 Same resolution experiment

The elements used in this experiment are: a microscope objective corrected to infinity with $f_{MO} = 9mm$ and $NA_{MO} = 0.4$ and $\phi_{AS} = 7.1mm$; the relay system composed of RL1 and RL2 with equal focal length of $f_1 = f_2 = 50mm$; the same MLA and sensor of section 3.1. In this case now we have N=7.1 which leads to a resolution of $\rho_{FiMic} = 6.1\mu m$ and $DOF_{FiMic} = 240\mu m$. Central views are shown in . 3, here the test was displaced up to $Z = \pm 110\mu m$. At Z=0 m both configuration resolve up to $6.2\mu m$ that is the element 3 of group 7. The DOF is established with a decrease in resolution of a factor $1/\sqrt{2}$, that is to say until element 6 of group 6. So, from Fig.2-(b) it is possible to see that the DOF of iMic extends to $80\mu m$ and for FiMic up to $220\mu m$, with a 2.75 times higher DOF in this case where resolution at the ROP is the same.

3.3 Orthographic views

Apart from the superior performances obtained, the important novelty of FiMic over iMic is the direct capture of the EIs. That simplifies the work of microscopists when choosing the position of the focus and the portion of the specimen to be within the DOF. With iMic, instead, the position of the focus needs to be guessed, and only after the computation of the views (EIs), from the capture, it can be confirmed. If not, another iteration of capture and computation will be needed, until reaching the desired result. In this sense it is more user-friendly the use of FiMic, especially in cases where in-vivo specimens are observed. An example of what is seen through both cameras is shown in Fig.3. On the left it is the specimen as seen with a FiMic, and on the right as seen through iMic. It is easy to asses that sensor images of FiMic are what we expect to see from an imaging system, whilst what is captured by iMic is more difficult to predict, even though after computational rearrangement of pixels also iMic provides the desired EIs. Nevertheless, it is this less step of computational work required by FiMic that makes it more easy to use it.

3.4 Focus plane selection, or refocusing

Once the EIs are obtained, many algorithms can be applied, one of the most interesting ones is the possibility to change the focus after taking the shot. One simple implementation of this algorithm is the shift and sum,[8] for FiMic the refocusing distance from the ROP, depends on the number n of shifted pixels and is calculated by

$$Z_R = n\frac{f_M^2 O}{f_L}\left(\frac{f_2}{f_1}\right)^2\frac{\delta}{p} \tag{8}$$

One feature that is important to underline is that differently than iMic, in FiMic all the refocused planes in the DOF maintain the same resolution as it is possible to see in Fig.4.

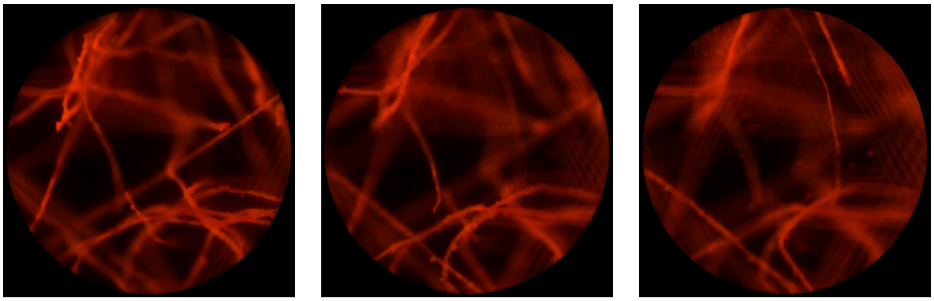

Figure 4. Refocusing capabilities of FIMic. FIMic preserve the same resolution along the entire DOF.

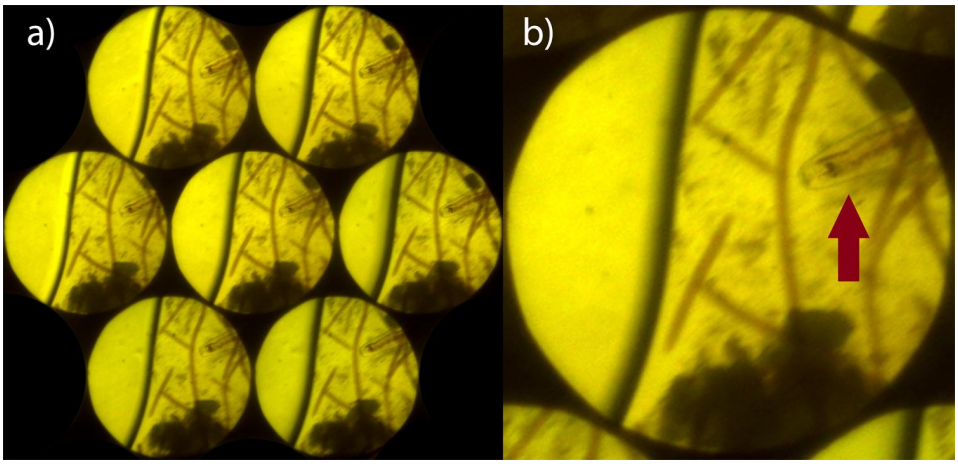

Figure 5. One frame of a video captured with N=3 in FiMic. a) shows the EIs. b) is a zoom of the central view with a red arrow pointing the marine nematode.

4. EXAMPLE OF IN-VIVO APPLICATION

Here, focusing on FiMic we want to propose some captures obtained with in-vivo samples. It has been possible thanks to the user-friendly capabilities of the system that allows to directly see the different perspectives (in this case N=3) and easily choose the position of the sample to focus on. Fig.5 shows one frame of a video captured with FiMic. On the left side all the perspectives are shown, and on the right a zoom in the central view to show the marine nematode (underlined by the red arrow) swimming through algae in see water. The great resolution of FiMic allows to see through the transparent membrane of the specimen, and internal details can be appreciated.

5. CONCLUSIONS

In this work we describe a Fourier plane integral microscope (FiMic). It is a 3D integral microscope that with a single sensor and a single shot is capable of sampling spatially and angularly the light-field. In comparison with the previous design, the iMic, we have proven that this setup allows improving by optic means the resolution and the DOF, allowing in-vivo recording of live specimens. This feature is enabled thanks to its more user-friendly direct-capture method. Finally, but not less important, this design can get really compact with a custom design, where only two optical elements are needed, the MO and the MLA, and an imaging sensor, to capture de information. Further work can be focused to retrieve with computational means more angular information, keeping the improved resolution.

ACKNOWLEDGMENTS

Some authors acknowledge their personal funding: E. Sanchez-Ortiga (APOSTD/ 2015/094); J. Sola-Pikabea (ACIF/2016/296); G. Scrofani (MSCA grant 676401); and A. Llavador (UVINV-PREDOC13-110484). J. Garcia-Sucerquia acknowledges the Universidad Nacional de Colombia for the Hermes grant 35765, and also to the University of Valencia for a Visiting Professor fellowship. Spanish Ministry of the Economy and Competitiveness (DPI2015-66458-C2-1R); GVA, Spain (PROMETEOII/2014/072).

REFERENCES

[1] G. Lippmann, "Epreuves reversibles donnant la sensation du relief," *J. Phys. Theor. Appl.*, vol. 7, no. 1, pp. 821–825, 1908.

[2] E. H. Adelson and J. Y. Wang, "Single lens stereo with a plenoptic camera," *IEEE transactions on pattern analysis and machine intelligence*, vol. 14, no. 2, pp. 99–106, 1992.

[3] J.-S. Jang and B. Javidi, "Three-dimensional integral imaging of micro-objects," *Optics letters*, vol. 29, no. 11, pp. 1230–1232, 2004.

[4] M. Levoy, R. Ng, A. Adams, M. Footer, and M. Horowitz, "Light field microscopy," in *ACM Transactions on Graphics (TOG)*, vol. 25, pp. 924–934, ACM, 2006.

[5] A. Llavador, E. Sánchez-Ortiga, J. C. Barreiro, G. Saavedra, and M. Martínez-Corral, "Resolution enhancement in integral microscopy by physical interpolation," *Biomedical optics express*, vol. 6, no. 8, pp. 2854–2863, 2015.

[6] A. Llavador, J. Sola-Pikabea, G. Saavedra, B. Javidi, and M. Martínez-Corral, "Resolution improvements in integral microscopy with fourier plane recording," *Optics express*, vol. 24, no. 18, pp. 20792–20798, 2016.

[7] M. Pluta and P. Maksymilian, *Advanced light microscopy*, vol. 1. Elsevier Amsterdam, 1988.

[8] S.-H. Hong, J.-S. Jang, and B. Javidi, "Three-dimensional volumetric object reconstruction using computational integral imaging," *Optics Express*, vol. 12, no. 3, pp. 483–491, 2004.